Hydrogen Bonding and Isomerism Arising from the Coordination Modes of Bridging Benzimidazole-2-thiolate Ligands in Tetranuclear Rhodium Complexes

Cristina Tejel,[†] B. Eva Villarroya,[†] Miguel A. Ciriano,*[,†] Andrew J. Edwards,[†] Fernando J. Lahoz,[†] Luis A. Oro,*[,†] Maurizio Lanfranchi,[‡] Antonio Tiripicchio,[‡] and Marisa Tiripicchio-Camellini[‡]

Departamento de Química Inorgánica, ICMA, Universidad de Zaragoza-CSIC, E−50009 Zaragoza, Spain, and Dipartimento di Chimica Generale ed Inorganica, Chimica Analitica, Chimica Fisica, Centro di Studio per la Strutturistica Diffrattometrica del CNR, Università di Parma, Viale delle Scienze 78, I-43100 Parma, Italy

Received October 31, 1997

Reaction of the dinuclear complex $[Rh_2(\mu\text{-HBzimt})_2(cod)_2]$ with $[Rh_2(\mu\text{-Cl})_2(cod)_2]$ (cod = 1,5-cyclooctadiene) gives the neutral tetranuclear complex $[Rh_4(\mu\text{-HBzimt})_2Cl_2(cod)_4]$ (**2**) in dichloromethane and the trinuclear cationic complex $[Rh_3(\mu\text{-HBzimt})_2(cod)_3]Cl$ (**3**) in methanol, respectively. The ionization ability of the solvent seems to be the driving force to give **3**, while the ability to coordinate a further RhCl(cod) fragment leads to **2** in poorer ionizing media. The complexes $[M_4(\mu\text{-HBzimt})_2Cl_2(diolefin)_4]$ (M = Rh, diolefin = tetrafluorobenzobarrelene (tfbb) (**5**); M = Ir, diolefin = cod (**6**)), formally analogous to **2**, were isolated from the reactions of the appropriate complexes [MCl(H_2Bzimt)(diolefin)] and [M(acac)(diolefin)] in acetone. A X-ray diffraction study on **2** shows the HBzimt$^-$ ligands to bridge two rhodium atoms through the sulfurs, forming a basic four-membered $Rh_2(\mu\text{-}(1{:}2\kappa S)\text{-HBzimt})_2$ ring along with two RhCl(cod) moieties bonded to the nitrogen atoms. Two intramolecular hydrogen bonds between the chloro ligands and the acidic NH protons should stabilize the syn-endo disposition of the thiolate type bridging ligands. Replacement of the olefin in **2** by carbon monoxide gives $[Rh_4(\mu\text{-HBzimt})_2Cl_2(cod)(CO)_6]$ and $[Rh_4(\mu\text{-HBzimt})_2Cl_2(CO)_8]$ (**7**) depending on the reaction conditions. The X-ray structure of **7** shows the HBzimt$^-$ ligands in a HT-$Rh_2(\mu\text{-}(1\kappa N,2\kappa S)\text{-HBzimt})_2$ disposition with two $RhCl(CO)_2$ fragments coordinated to the sulfur atoms. In addition, two tetranuclear units **7** are associated in a dimer through four intermolecular hydrogen bonds. This association occurs even in solution, where the two species are observed. The equilibrium constant for the dissociation fits a linear plot of ln K_{eq} versus $1/T$, which gives $\Delta H = 43.3$ kJ mol^{-1} and $\Delta S = 114.7$ J K^{-1} mol^{-1}. Deprotonation of **7** with $[Rh_2(\mu\text{-OMe})_2(cod)_2]$ gives the hexanuclear complex $[Rh_6(\mu\text{-Bzimt})_2(\mu\text{-Cl})_2(cod)_2(CO)_8]$ (**10**). Complexes **7** and **10** show identical conformations of the eight-membered HT-$Rh_2(\mu\text{-}(1\kappa N,2\kappa S)\text{-Bzimt})_2$ metallacycle and identical configurations of the sulfur atoms.

Introduction

As part of our current investigations[1] into the chemistry of polynuclear complexes containing anionic ligands of the N−C−X (X = N, O, S) type, we recently reported the stepwise construction of a new family of di-, tri-, and tetranuclear complexes[2] using the deprotonated forms of 2-mercaptobenzimidazole (H_2Bzimt) as backbones to hold M(cod) moieties (M = Rh, Ir; cod = 1,5-cyclooctadiene) in close proximity. All these polynuclear complexes, and most of those reported with pyridine-2-thiolate (Pyt), benzothiazole-2-thiolate (Bztzt), and related ligands, show a basic eight-membered $M_2(\mu\text{-}(1\kappa N,2\kappa S)_2)$ ring with the two bridging ligands arranged in HT (head-to-tail) or HH (head-to-head) dispositions, as found for rhodium and iridium dinuclear complexes[3] (A, Figure 1). This binucleating mode, through the N and the S atoms, seems to be the most usual for these and other related N−C−S type ligands bridging transition metals such as Pd,[4] Pt,[5] Ru,[6] and Os,[7]

[†] Universidad de Zaragoza.
[‡] Università di Parma.

(1) (a) Pérez-Torrente, J. J.; Casado, M. A.; Ciriano, M. A.; Lahoz, F. J.; Oro, L. A. *Inorg. Chem.* **1996**, *35*, 1782. (b) Villarroya, B. E.; Oro, L. A.; Lahoz, F. J.; Edwards, A. J.; Ciriano, M. A.; Alonso, P. J.; Tiripicchio, A.; Tiripicchio-Camellini, M. *Inorg. Chim Acta* **1996**, *250*, 241. (c) Ciriano, M. A.; Villarroya, B. E.; Oro, L. A.; Apreda, M. C.; Foces-Foces, C.; Cano, F. H. *J. Organomet. Chem.* **1989**, *266*, 377. (d) Ciriano, M. A.; Villarroya, B. E.; Oro, L. A.; Apreda, M. C.; Foces-Foces, C.; Cano, F. H. *J. Chem. Soc., Dalton Trans.* **1987**, 981. (e) Lahoz, F. J.; Viguri, F.; Ciriano, M. A.; Oro, L. A.; Foces-Foces, C.; Cano, F. H. *Inorg. Chim. Acta* **1987**, *128*, 119. (f) Oro, L. A.; Ciriano, M. A.; Viguri, F.; Tiripicchio, A.; Tiripicchio-Camellini, M.; Lahoz, F. J. *New J. Chem.* **1986**, *10*, 75. (g) Ciriano, M. A.; Oro, L. A.; Pérez-Torrente, J. J.; Tiripicchio, A.; Tiripicchio-Camellini, M. *J. Chem. Soc., Chem. Commun.* **1986**, 1737. (h) Oro, L. A.; Ciriano, M. A.; Villarroya, B. E.; Tiripicchio, A.; Lahoz, F. J. *J. Chem. Soc., Dalton Trans.* **1985**, 1891.

(2) Tejel, C.; Villarroya, B. E.; Ciriano, M. A.; Oro, L. A.; Lanfranchi, M.; Tiripicchio, A.; Tiripicchio-Camellini, M. *Inorg. Chem.* **1996**, *35*, 4360.

(3) (a) Ciriano, M. A.; Pérez-Torrente, J. J.; Lahoz, F. J.; Oro, L. A. *J. Organomet. Chem.* **1993**, *455*, 225. (b) Xiao, J.; Cowie, M. *Can. J. Chem.* **1993**, *71*, 726. (c) Ciriano, M. A.; Viguri, F.; Pérez-Torrente, J. J.; Lahoz, F. J.; Oro, L. A.; Tiripicchio, A.; Tiripicchio-Camellini, M. *J. Chem. Soc., Dalton Trans.* **1989**, 25. (d) Sielisch, T.; Cowie, M. *Organometallics* **1988**, *7*, 707. (e) Ciriano, M. A.; Sebastián, S.; Oro, L. A.; Tiripicchio, A.; Tiripicchio-Camellini, M.; Lahoz, F. J. *Angew. Chem., Int. Ed. Engl.* **1988**, *27*, 402. (f) Lifsey, R. S.; Chavan, M. Y.; Chau, L. K.; Ahsan, M. Q.; Kadish, K. M.; Dear, J. L. *Inorg. Chem.* **1987**, *26*, 822. (g) Deeming, A. J.; Meah, M. N. N.; Dawes, H. M.; Hursthouse, M. B. *J. Organomet. Chem.* **1986**, *299*, C25.

(4) (a) Gupta, M. G.; Cramer, R. E.; Ho, K.; Pettersen, C.; Mishina, S.; Belli, J.; Jensen, C. M. *Inorg. Chem.* **1995**, *34*, 60. (b) Engelking, H.; Karentzopoulos, S.; Reusmann, G.; Krebs, B. *Chem. Ber.* **1994**, *127*, 2355. (c) Yap, G. P. A.; Jensen, C. M. *Inorg. Chem.* **1992**, *31*, 4823.

S0020-1669(97)01376-1 CCC: $15.00
Published on Web 07/17/1998

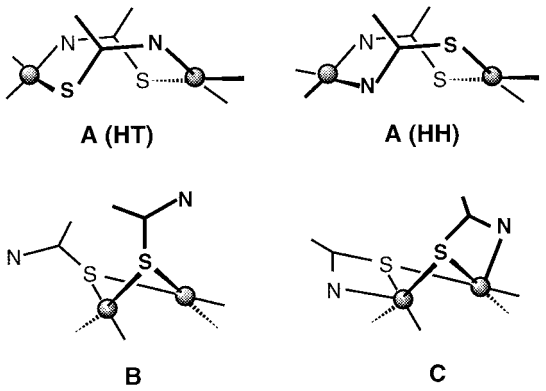

Figure 1. Coordination modes of benzimidazole-2-thionate (HBzimt$^-$) in dinuclear complexes.

probably due to a delocalization of the negative charge in the N−C−S bonds. A localization of the charge in both bridging ligands on the sulfur atoms would lead to the formation of a four-membered $M_2(\mu\text{-}(1{:}2\kappa S)_2)$ ring similar to that found for dinuclear organothiolate complexes[8] (B, Figure 1). Although the ligands of the N−C−S type could allow this type of coordination, a search on the Cambridge Data Base for the $M_2(S)_2$ metallacycle, formed from the N−C−S ligands and metals, revealed that only two similar trinuclear complexes[7a,9] of Ru and Os with pyridine-2-thiolate show a "pure" organothiolato coordination. The structures showing N−C−S ligands bridging through the sulfur atoms are systematically associated with a chelate ring NCS−M involving both the sulfur and nitrogen atoms, which results in a μ-(1κN,1:2κS) coordination mode (C, Figure 1).[10]

We describe in this paper the first tetranuclear complex with two bridging N−C−S ligands showing a μ-(1:2κS) coordination mode, which undergoes a change in the μ-(1κN,2κS) coordination mode by replacement of the ancillary ligands. We also give evidence of conformational changes of the $M_2(\mu\text{-}(1\kappa N,2\kappa S)_2)$ dimetallacycle and migrations of the metal centers in these complexes.

Results and Discussion

Syntheses and Transformations of the Tetranuclear Complexes $[M_4(\mu\text{-HBzimt})_2Cl_2(\text{diolefin})_4]$ (M = Rh, diolefin = cod, tfbb; M = Ir, diolefin = cod). Reaction of $[Rh_2(\mu\text{-HBzimt})_2(cod)_2]$ (**1**) with $[Rh_2(\mu\text{-Cl})_2(cod)_2]$ (1:1 molar ratio)

Scheme 1[a]

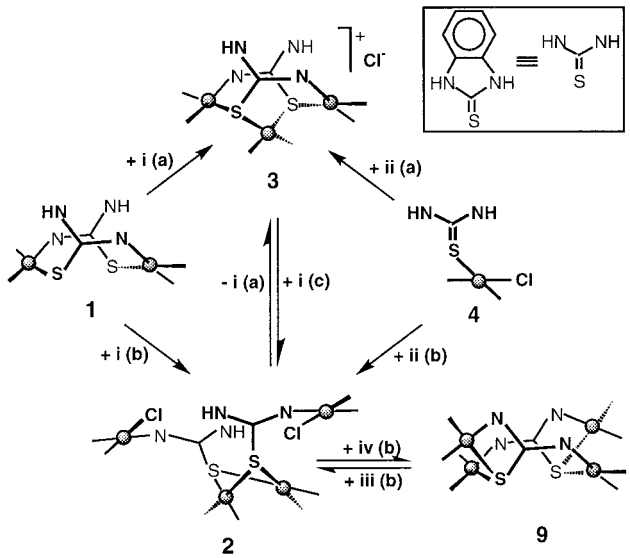

[a] Key: (i) $[M_2(\mu\text{-Cl})_2(\text{diolefin})_2]$; (ii) [M(acac)(diolefin)]; (iii) HCl; (iv) KOH; (a) methanol; (b) acetone; (c) dichloromethane. Shaded ○< represents the M(cod) moiety. Simple skeletal views of the complexes are shown.

(cod = 1,5-cyclooctadiene) in acetone gives an air-stable red solid characterized as the unexpected tetranuclear complex $[Rh_4(\mu\text{-HBzimt})_2Cl_2(cod)_4]$ (**2**). Thus, the IR and ^{1}H NMR spectra show the ν(N−H) band and a low-field resonance for the NH protons, respectively, and the analytical data, including the molecular weight in chloroform, are consistent with the proposed formula. More surprisingly, an X-ray diffraction study on **2** (vide infra) shows the HBzimt$^-$ ligands to bridge two rhodium atoms through the sulfurs, forming a basic four-membered $Rh_2(\mu\text{-}(1{:}2\kappa S)\text{-HBzimt})_2$ ring along with two RhCl(cod) moieties bonded to the nitrogen atoms. When the reaction between **1** and $[Rh_2(\mu\text{-Cl})_2(cod)_2]$ is carried out under identical conditions but in methanol, the trinuclear ionic complex $[Rh_3(\mu\text{-HBzimt})_2(cod)_3]Cl$ (**3**) crystallizes out as a purple solid (Scheme 1). Unreacted $[Rh_2(\mu\text{-Cl})_2(cod)_2]$ remains in solution. Complex **3** exists as a static single isomer in CD_3OD solution. The structure, determined by ^{1}H, ^{13}C{^{1}H}, and H−H COSY NMR spectra, contains the basic eight-membered HT-$Rh_2(\mu\text{-}(1\kappa N,2\kappa S)\text{-HBzimt})_2$ ring of the dinuclear complex **1** to which the third Rh(cod) moiety is chelated through the two sulfur atoms, as previously described.[2]

Complexes **2** and **3** are thus related by the loss or addition of one RhCl(cod) fragment and ionization of chloride. These reactions can be shifted almost quantitatively either in one or in the opposite direction by the use of the appropriate solvent. Thus, red crystals of **2** dissolve in methanol slowly to give purple crystals of **3** and a yellow solution containing $[Rh_2(\mu\text{-Cl})_2(cod)_2]$ (^{1}H NMR evidence). Further evaporation of the solvent and addition of dichloromethane to the residue give a red solution from which complex **2** is recovered in good yield (see Scheme 1). Moreover, complex **3** slowly dissolves in dichloromethane to give an equimolecular mixture of **1** and **2** according to eq 1.

$$2[\underset{\mathbf{3}}{Rh_3(\mu\text{-HBzimt})_2(cod)_3}]Cl \rightleftharpoons [\underset{\mathbf{1}}{Rh_2(\mu\text{-HBzimt})_2(cod)_2}] + [\underset{\mathbf{2}}{Rh_4(\mu\text{-HBzimt})_2Cl_2(cod)_4}] \quad (1)$$

The formation of **2** and **3** should proceed through the initial bridge cleavage of $[Rh_2(\mu\text{-Cl})_2(cod)_2]$ by the dinuclear complex

(d) Umakoshi, K.; Ichimura, A.; Kinoshita, I.; Ooi, S. *Inorg. Chem.* **1990**, *29*, 4005. (e) Kubiak, M. *Acta Crystallogr., C* **1985**, *41*, 1288.
(5) (a) Umakoshi, K.; Kinoshita, I.; Fukui-Yasuba, Y.; Matsumoto, K.; Ooi, S.; Nakai, H.; Shiro, M. *J. Chem. Soc., Dalton Trans.* **1989**, 815. (b) Goodgame, D. M. L.; Rollins, R. W.; Slawin, A. M. Z.; Williams, D. J.; Zard, P. W. *Inorg. Chim. Acta* **1986**, *120*, 91.
(6) (a) Sherlock, S. J.; Cowie, M.; Singleton, E.; Steyn, M. M. d. V. *J. Organomet. Chem.* **1989**, *361*, 353. (b) Jeannin S.; Jeannin, Y.; Lavigne, G. *Transition Met. Chem.* **1976**, *1*, 186.
(7) (a) Deeming, A. J.; Vaish, R.; Arce, A. J.; de Sanctis, Y. *Polyhedron* **1994**, *13*, 3285. (b) Zhang N.; Wilson, S. R.; Shapley, P. A. *Organometallics* **1988**, *7*, 1126.
(8) (a) Ciriano, M. A.; Pérez-Torrente, J. J.; Lahoz, F. J.; Oro, L. A. *J. Chem. Soc., Dalton Trans.* **1992**, 1831. (b) Bonnet, J. J.; Kalck, P.; Poilblanc, R. *Inorg. Chem.* **1988**, *27*, 2131. (c) Cotton, F. A.; Lahuerta, P.; LaTorre, J.; Sanau, M.; Solana, I.; Schwotzer, W. *Inorg. Chem.* **1988**, *27*, 2131.
(9) Au, Y.-K.; Cheung, K.-K.; Wong, W.-T. *Inorg. Chim. Acta* **1995**, *228*, 267.
(10) (a) Landgrafe, C.; Sheldrick, W. D. *J. Chem. Soc., Dalton Trans.* **1996**, 989. (b) Ciriano, M. A.; Pérez-Torrente, J. J.; Lahoz, F. J.; Oro, L. A. *J. Organomet. Chem.* **1994**, *482*, 53. (c) Sheldrick, W. S.; Landgrafe, C. *Inorg. Chim. Acta* **1993**, *208*, 145. (d) Deeming, A. J.; Hardcastle, K. I.; Harim, M. *Inorg. Chem.* **1992**, *31*, 4792.

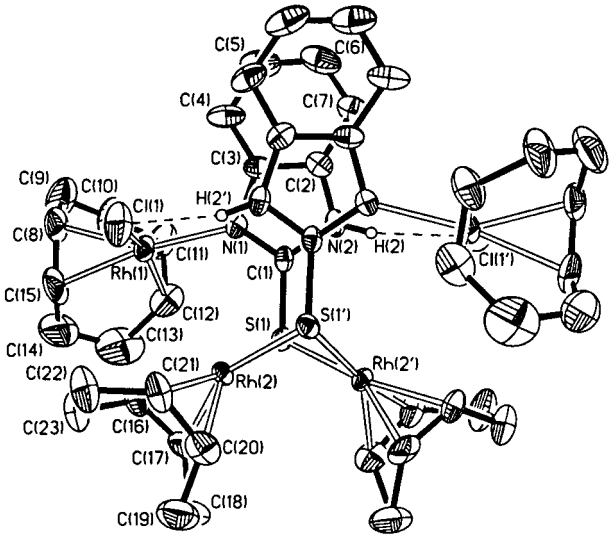

Figure 2. ORTEP view of the structure of the complex $[Rh_4(\mu\text{-HBzimt})_2Cl_2(cod)_4]$ (**2**). The ellipsoids for the atoms are drawn at the 30% probability level.

1 to give a trinuclear intermediate $[Rh_3(\mu\text{-HBzimt})_2Cl(cod)_3]$, where the RhCl(cod) group is bonded to a sulfur atom. An interaction of this Rh with the second sulfur atom to form the chelate ring, along with the ionization of the chloro ligand, gives **3** in methanol. Complex **3** could also be formed in dichloromethane or acetone, but either association of the ionic chloride in **3** to one of the Rh atoms coordinated through S and N or the transfer of the chloro ligand to a close metal in the intermediate breaks the Rh−S bond, allowing the coordination of a second RhCl(cod) moiety to this terminal sulfur. A further transfer of chloride repeating the above step renders complex **2** with the observed structure in the solid state.

The high ionization ability of the solvent seems to be the driving force to give **3** independently of the molar ratio, while the ability to coordinate a further RhCl(cod) leads to **2** in poorer ionizing media. Thus, the alternative synthesis of **2** or **3** by condensation between the mononuclear complexes [RhCl(H_2-Bzimt)(cod)] (**4**) and [Rh(acac)(cod)] (1:1 molar ratio) (Scheme 1) gives complex **3** and unreacted [Rh(acac)(cod)] from methanolic solutions, but complex **2** from acetone solutions. Using this method, the complexes $[M_4(\mu\text{-HBzimt})_2Cl_2(diolefin)_4]$ (M = Rh, diolefin = tetrafluorobenzobarrelene (tfbb) (**5**); M = Ir, diolefin = cod (**6**)) were isolated from the reactions of the appropriate complexes [MCl(H_2Bzimt)(diolefin)] and [M(acac)-(diolefin)] in acetone. Complexes **5** and **6** are green air-stable solids, but remarkably, **6** spontaneously loses HCl upon solution in $CDCl_3$ to give the already known red complex $[Ir_4(\mu\text{-Bzimt})_2(cod)_4]$.

Crystal Structure of the Complex $[Rh_4(\mu\text{-HBzimt})_2Cl_2(cod)_4]$ (2). The structure of complex **2** is shown in Figure 2 together with the atom-numbering scheme. Selected bond distances and angles are given in Table 1. In the tetranuclear complex **2**, having a crystallographic imposed C_2 symmetry, each Rh atom is bound to a cod molecule through the two olefinic double bonds. The four metal atoms are connected through two monodeprotonated HBzimt$^-$ anions, each of which acts as bidentate ligand, bridging two Rh atoms through the S atom and being bound to a third Rh atom through the deprotonated N atom. If the midpoints of the two double bonds of each cod molecule are considered as coordination sites, each Rh atom displays a distorted square planar coordination. The four Rh complexes can be considered of two types: the former

Table 1. Selected Bond Distances (Å) and Angles (deg) for Complex **2**

Rh(1)−Cl(1)	2.393(2)	S(1)−Rh(2′)[a]	2.394(2)
Rh(1)−N(1)	2.102(4)	S(1)−C(1)	1.753(5)
Rh(1)−C(8)	2.115(6)	N(1)−C(1)	1.323(7)
Rh(1)−C(11)	2.123(8)	N(1)−C(3)	1.394(7)
Rh(1)−C(12)	2.101(8)	N(2)−C(1)	1.354(7)
Rh(1)−C(15)	2.139(7)	N(2)−C(2)	1.390(7)
Rh(2)−S(1)	2.405(2)	C(2)−C(3)	1.398(8)
Rh(2)−C(16)	2.155(6)	C(8)−C(15)	1.369(12)
Rh(2)−C(17)	2.148(7)	C(11)−C(12)	1.397(11)
Rh(2)−C(20)	2.124(7)	C(16)−C(17)	1.375(9)
Rh(2)−C(21)	2.129(7)	C(20)−C(21)	1.375(9)
C(12)−Rh(1)−C(15)	81.8(3)	S(1)−Rh(2)−C(17)	87.4(2)
C(11)−Rh(1)−C(15)	90.9(3)	S(1)−Rh(2)−C(16)	98.1(2)
C(8)−Rh(1)−C(12)	96.9(3)	Rh(2)−S(1)−Rh(2′)	75.3(1)
C(8)−Rh(1)−C(11)	81.7(3)	Rh(2)−S(1)−C(1)	110.5(2)
N(1)−Rh(1)−C(12)	93.3(3)	C(1)−S(1)−Rh(2′)	112.0(2)
N(1)−Rh(1)−C(11)	90.1(2)	C(1)−N(1)−C(3)	106.5(4)
Cl(1)−Rh(1)−C(15)	93.3(3)	C(1)−N(2)−C(2)	107.7(5)
Cl(1)−Rh(1)−C(8)	91.9(2)	N(1)−C(1)−N(2)	111.7(5)
Cl(1)−Rh(1)−N(1)	88.3(1)	S(1)−C(1)−N(2)	124.5(4)
C(17)−Rh(2)−C(21)	96.9(3)	S(1)−C(1)−N(1)	123.5(4)
C(17)−Rh(2)−C(20)	81.9(3)	N(2)−C(2)−C(3)	105.5(5)
C(16)−Rh(2)−C(21)	81.6(3)	N(1)−C(3)−C(2)	108.6(5)
C(16)−Rh(2)−C(20)	90.1(3)		

[a] Prime = $1 - x, y, {}^1/_2 - z$.

completes its coordination through two S atoms from two HBzimt$^-$ anions; the latter, through the chlorine and N atoms. The complex can be described as consisting of a dimeric Rh_2-(μ-(1:2kS)-HBzimt)$_2$ fragment in which the deprotonated N atoms are bound to a RhCl(cod) moiety. In the dimeric fragment a four-membered Rh_2S_2 ring is present displaying a butterfly conformation (the dihedral angle between the two SRhS wings is 116.71(4)°). Noteworthy are the short Rh···Rh and S···S separations, 2.931(1) and 3.343(2) Å, respectively, indicative of weak interactions. The two HBzimt$^-$ anions show a syn-endo conformation and are practically parallel, as the dihedral angle between them is 2.58(4)°. Due to this diposition of the two anions, relevant stacking interactions can be envisaged: six separations, shorter than 3.50 Å, are present, the shortest one being 3.130(7) Å. The two S-bridges are symmetric, the Rh−S bond distances being 2.405(2) and 2.394-(2) Å; the Rh−N bond distances are quite normal, 2.102(4) Å. The C(1)−N(1) and C(1)−N(2) bond distances, 1.323(7) and 1.354(7) Å, respectively, are in agreement with a C−N double-bond delocalization.

The syn-endo isomer, even if less favored on steric grounds with respect to the syn-exo and anti isomers as detected by molecular models, is probably stabilized by two strong intramolecular hydrogen bonds involving the Cl atom and the N−H groups [N···Cl = 3.235(5) Å and H···Cl = 2.33(7) Å; N−H···Cl = 171(7)°] (Figure 3). The HBzimt$^-$ ligands are planar with the N-bound Rh atom almost coplanar.

The Linkage Isomerization Occurring in the Formation of the Tetranuclear Complex $[Rh_4(\mu\text{-HBzimt})_2Cl_2(CO)_8]$ (7). Bubbling carbon monoxide through a dichloromethane solution of $[Rh_4(\mu\text{-HBzimt})_2Cl_2(cod)_4]$ (**2**) gives a wine-red solution of the complex $[Rh_4(\mu\text{-HBzimt})_2Cl_2(CO)_8]$ (**7**). Isolation of **7** requires its crystallization under an atmosphere of carbon monoxide. Otherwise, a partial substitution of two carbonyl groups by the replaced cod occurs under an inert atmosphere to give pink needles of $[Rh_4(\mu\text{-HBzimt})_2Cl_2(cod)(CO)_6]$ (**8**). Complex **7** was characterized by spectroscopical means and by a single-crystal X-ray diffraction study as tetranuclear, containing a basic eight-membered HT-$Rh_2(\mu$-(1κN,2κS)-HBzimt)$_2$

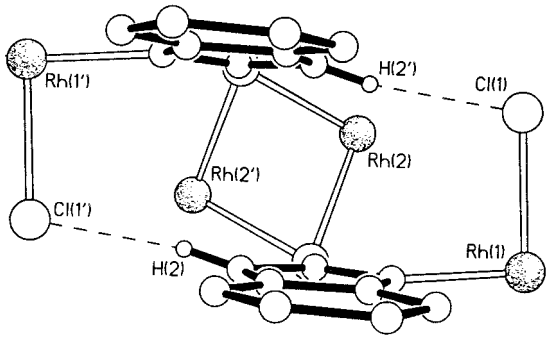

Figure 3. View of the bridging framework in **2** showing the hydrogen bonding.

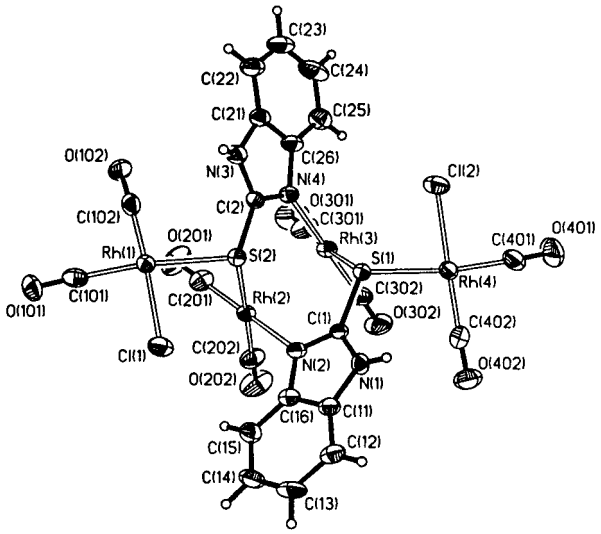

Figure 4. ORTEP view of the structure of the complex $[Rh_4(\mu\text{-HBzimt})_2Cl_2(CO)_8]$ (**7**). The ellipsoids for the atoms are drawn at the 30% probability level.

ring. However, complex **8** still seems to maintain the four-membered $Rh_2(\mu\text{-}(1{:}2\kappa S)\text{-HBzimt})_2$ ring present in the starting material, the cod ligand being coordinated to one of the bridged rhodium atoms (see below). Therefore, a change of the bridging mode of the $HBzimt^-$ ligands occurs just at the final step of the carbonylation reaction. An extraordinary change of the skeletal core also occurs on a deprotonation reaction of **2** (see Scheme 1). Thus, addition of 2 molar equiv of NEt_3 to an acetone suspension of **2** gives the known tetranuclear complex $[Rh_4(\mu\text{-Bzimt})_2(cod)_4]$ (**9**), having a basic eight-membered HT-$Rh_2(\mu\text{-}(1\kappa N,2\kappa S)\text{-Bzimt})_2$ ring. The reaction can be reversed on addition of 2 molar equiv of HCl to **9** in acetone, which regenerates **2** in quantitative yield.

Crystal Structure of the Complex $[Rh_4(\mu\text{-HBzimt})_2Cl_2(CO)_8]$ (7). The structure of the complex **7** is shown in Figure 4 together with the atom-numbering scheme. Selected bond distances and angles are given in Table 2. Complex **7** shows an approximate C_2 symmetry. The four metal atoms are connected through two monodeprotonated $HBzimt^-$ anions, each of which acts as a bidentate ligand, bridging two Rh atoms through the S atom and being bound to a third Rh atom through the deprotonated N atom. The complex can be described as consisting of a dimeric $Rh_2(\mu\text{-}(1\kappa N,2\kappa S)\text{-HBzimt})_2$ fragment in which two $HBzimt^-$ ligands bridge the two Rh atoms in a head-to-tail (HT) disposition. These Rh atoms complete their square planar coordination with two carbonyl ligands. Moreover, two $RhCl(CO)_2$ fragments are bound to the sulfur atoms, to form the tetranuclear Rh complex. In the dimeric fragment an eight-membered $Rh_2S_2C_2N_2$ ring is present in which a short Rh···Rh separation, 2.984(1) Å, can be envisaged. This ring shows two planar SCNRh moieties and can be described as formed by two "envelope" five-membered rings sharing the Rh···Rh side. The four Rh−S bond distances, in the range 2.375(2)−2.401(2) Å, and the two Rh−N ones, 2.086(5) and 2.088(5) Å, are comparable to those found in complex **2**. An extensive double bond delocalization on the N−C−N moiety is observed as in **2**.

Table 2. Selected Bond Distances (Å) and Angles (deg) for Complex **7**

Rh(1)−Cl(1)	2.354(2)	Rh(4)−Cl(2)	2.348(2)
Rh(1)−S(2)	2.380(2)	Rh(4)−S(1)	2.375(2)
Rh(1)−C(101)	1.862(7)	Rh(4)−C(401)	1.868(7)
Rh(1)−C(102)	1.843(6)	Rh(4)−C(402)	1.844(7)
Rh(2)−S(2)	2.392(1)	Rh(3)−S(1)	2.401(2)
Rh(2)−N(2)	2.086(5)	Rh(3)−N(4)	2.088(5)
Rh(2)−C(201)	1.866(7)	Rh(3)−C(301)	1.875(7)
Rh(2)−C(202)	1.875(7)	Rh(3)−C(302)	1.859(7)
S(1)−C(1)	1.748(6)	S(2)−C(2)	1.748(6)
N(1)−C(1)	1.345(8)	N(3)−C(2)	1.346(8)
N(1)−C(11)	1.370(8)	N(3)−C(21)	1.391(8)
N(2)−C(1)	1.334(7)	N(4)−C(2)	1.322(7)
N(2)−C(16)	1.392(7)	N(4)−C(26)	1.408(7)
C(11)−C(16)	1.395(9)	C(21)−C(26)	1.378(9)
C(101)−O(101)	1.132(8)	C(301)−O(301)	1.121(9)
C(102)−O(102)	1.133(8)	C(302)−O(302)	1.127(9)
C(201)−O(201)	1.129(9)	C(401)−O(401)	1.123(9)
C(202)−O(202)	1.127(9)	C(402)−O(402)	1.139(9)
C(101)−Rh(1)−C(102)	90.6(3)	C(401)−Rh(4)−C(402)	90.6(3)
S(2)−Rh(1)−C(102)	96.4(2)	S(1)−Rh(4)−C(402)	97.4(2)
S(2)−Rh(1)−C(101)	172.8(2)	S(1)−Rh(4)−C(401)	171.7(2)
Cl(1)−Rh(1)−C(102)	174.0(2)	Cl(2)−Rh(4)−C(402)	177.8(2)
Cl(1)−Rh(1)−C(101)	86.1(2)	Cl(2)−Rh(4)−C(401)	88.1(2)
Cl(1)−Rh(1)−S(2)	86.7(1)	Cl(2)−Rh(4)−S(1)	83.9(1)
C(201)−Rh(2)−C(202)	90.9(3)	C(301)−Rh(3)−C(302)	91.2(3)
N(2)−Rh(2)−C(202)	92.1(3)	N(4)−Rh(3)−C(301)	90.2(3)
N(2)−Rh(2)−C(201)	176.9(3)	N(4)−Rh(3)−C(302)	178.5(3)
S(2)−Rh(2)−C(202)	175.7(2)	S(1)−Rh(3)−C(301)	175.3(2)
S(2)−Rh(2)−C(201)	91.9(2)	S(1)−Rh(3)−C(302)	90.9(2)
S(2)−Rh(2)−N(2)	85.1(1)	S(1)−Rh(3)−N(4)	87.7(1)
Rh(3)−Rh(2)−C(202)	100.5(2)	Rh(2)−Rh(3)−C(301)	100.7(2)
Rh(3)−Rh(2)−C(201)	94.8(2)	Rh(2)−Rh(3)−C(302)	94.1(2)
Rh(3)−Rh(2)−N(2)	85.8(1)	Rh(2)−Rh(3)−N(4)	85.3(1)
Rh(3)−Rh(2)−S(2)	82.5(1)	Rh(2)−Rh(3)−S(1)	83.3(1)
Rh(3)−S(1)−Rh(4)	103.5(1)	Rh(1)−S(2)−Rh(2)	99.7(1)
Rh(4)−S(1)−C(1)	113.3(2)	Rh(1)−S(2)−C(2)	113.2(2)
Rh(3)−S(1)−C(1)	107.3(2)	Rh(2)−S(2)−C(2)	105.6(2)
C(1)−N(1)−C(11)	108.6(5)	C(2)−N(3)−C(21)	108.9(5)
Rh(2)−N(2)−C(16)	125.5(4)	Rh(3)−N(4)−C(26)	127.8(4)
Rh(2)−N(2)−C(1)	126.8(4)	Rh(3)−N(4)−C(2)	126.2(4)
C(1)−N(2)−C(16)	106.4(5)	C(2)−N(4)−C(26)	105.9(5)

The mean coordination planes of the two central Rh atoms are almost parallel (the dihedral angle is 16.54(9)° and are almost perpendicular to those of the two external Rh atoms (the dihedral angles between adjacent complexes are 87.40(7) and 86.92(7)°).

The tetranuclear complexes **7** are associated in dimeric complexes, having C_2 symmetry, through four NH···Cl hydrogen bonds [N(3)···Cl(1′) = 3.1342(6) Å and H···Cl(1′) = 2.41(7) Å; N(3)−H···Cl(1′) = 173(8)°; [N(1)···Cl (2′) = 3.205(5) Å and H···Cl(2′) = 2.47(6) Å; N(1)−H···Cl(2′) = 158(5)° (the apex refers to the transformation $-x$, $^1/_2-y$, z)] and two very weak Rh···Rh interactions [Rh(1)···Rh(1′) = 3.556(1) and Rh(4)···Rh(4′) = 3.619(1) Å]. The octanuclear complex is shown in Figure 5.

Synthesis and X-ray Structure of the Hexanuclear Complex $[Rh_6(\mu\text{-Bzimt})_2(\mu\text{-Cl})_2(cod)_2(CO)_8]$ (10). Complex **7** still has two acidic hydrogens that are abstracted by $[Rh_2(\mu\text{-OMe})_2(cod)_2]$ in dichloromethane, leading to a red solid characterized

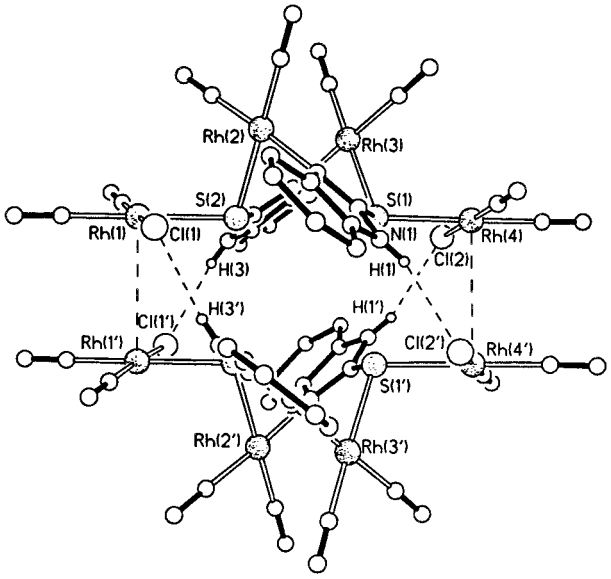

Figure 5. A pair of complexes **7** associated in dimers through four NH···Cl hydrogen bonds and two weak Rh···Rh interactions.

Chart 1. Possible Structures for the Complex $[Rh_6(\mu\text{-Bzimt})_2(\mu\text{-Cl})_2(cod)_2(CO)_8]$ (**10**)[a]

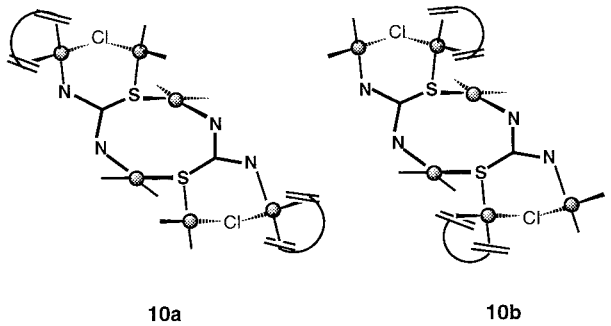

10a **10b**

[a] Shaded ○< represents the $Rh(CO)_2$ moiety.

as the hexanuclear complex $[Rh_6(\mu\text{-Bzimt})_2(\mu\text{-Cl})_2(cod)_2(CO)_8]$ (**10**). The reaction takes place cleanly to give one single isomer. As the addition of two new fragments Rh(cod) occurs along with the deprotonation, one can think that they bind **7** through the deprotonated nitrogen and an additional chloro ligand to give **10a**, as shown in Chart 1. However, the X-ray diffraction study on **10** revealed the formation of the related isomer (labeled **10b** in Chart 1). The structure of the complex **10** is shown in Figure 6 together with the atom-numbering scheme. Selected bond distances and angles are given in Table 3. The hexanuclear complex **10** shows a pseudo C_2 symmetry (in the Figure 6 the primed atoms indicate the approximately related ones), and three different square planar Rh complexes are present. The six metal atoms are connected through two bideprotonated $Bzimt^{2-}$ anions, each of which acts as a tridentate ligand, bridging two Rh atoms through the S atom and being bound to two Rh atoms through both deprotonated N atoms. The complex is very similar to complex **7** with a dimeric $Rh_2(\mu\text{-}(1\kappa N,2\kappa S)\text{-Bzimt})_2$ fragment in which two $HBzimt^-$ ligands bridge the two Rh atoms in a head-to-tail (HT) disposition through the S(1) and N(2) atoms. These Rh atoms complete their square planar coordination with two carbonyl ligands. Moreover, two RhCl(cod) fragments are bound to the sulfur atoms, to form a tetranuclear Rh complex. The mean coordination planes of the two central Rh atoms are almost parallel as in **7** (the dihedral angle is 17.17(8)°). The deprotonated N(1) atom interacts with

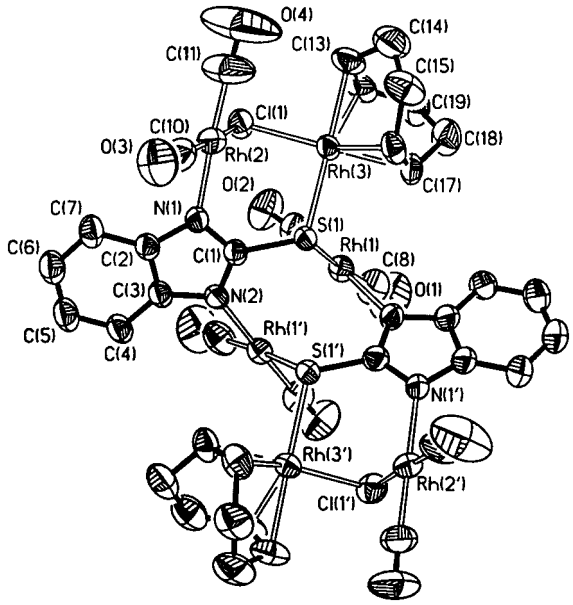

Figure 6. ORTEP view of the structure of the complex $[Rh_6(\mu\text{-Bzimt})_2(\mu\text{-Cl})_2(cod)_2(CO)_8]$ (**10**). The ellipsoids for the atoms are drawn at the 30% probability level.

another $Rh(CO)_2Cl$ fragment in order to obtain the hexanuclear complex in which the Cl atoms bridge two Rh atoms with formation of six-membered RhClRhSCN rings.

In the dimeric fragment an eight-membered $Rh_2S_2C_2N_2$ ring, very similar to that found in **7**, is present in which a comparable short Rh···Rh separation, 2.998(1) Å, is found.

For complex **10**, the structure found in the solid state is maintained in solution according to analytical and spectroscopic data. Thus, the molecular weight in chloroform solution corresponds to the hexanuclear complex. The ^1H NMR spectrum in $CDCl_3$ is consistent with a nonfluxional molecule showing one type of $Bzimt^{2-}$ ligand and 12 resonances for the protons of the two equivalent cod ligands (confirmed by the H−H COSY spectrum), in accordance with the C_2 symmetry of **10**. This symmetry is again observed from the $^{13}C\{^1H\}$ NMR spectrum, which shows four doublets ($J_{Rh-C} = 62-80$ Hz) for the CO groups and four doublets ($J_{Rh-C} = 11-16$ Hz) and four singlets for the olefinic and methylenic carbons of the cod ligands, respectively, together with six resonances in the aromatic region for the two equivalent $Bzimt^{2-}$ ligands. Both spectra are static, which should be attributed to an ensemble of factors working together: the lack of acidic hydrogen, the bridging nature of the chloro ligands, and the system of three fused rings that provides a conformational rigidity.

Structures and Behaviors of the Tetranuclear Complexes 2, 5, 7, and 8 in Solution. Intra- and Intermolecular Hydrogen Bonding. Complexes **2** and **7** give red solutions in $CDCl_3$ whose ^1H NMR spectra show the presence of two compounds (**2a**/**2b** and **7a**/**7b**), while complexes **5** and **8** each exist as a single isomer in solution. The representative signals in the ^1H NMR spectrum of complexes **2a**/**2b** (ca. in 9:1 molar ratio) are one broad singlet for the HN protons, four resonances due to the H^3-H^6 protons of the $HBzimt^-$ ligands, and eight multiplets for the olefinic protons of the cod ligands, which slightly broaden at room temperature. Analysis of the H−H COSY spectrum of **2a** and **2b** at low temperature indicates that the bridging ligands are equivalent and there are two pairs of equivalent cod ligands in both complexes. Thus, **2a** and **2b** (Scheme 2) possess a C_2 symmetry axis, which excludes HH

Table 3. Selected Bond Distances (Å) and Angles (deg) for Complex **10**

Rh(1)−S(1)	2.388(1)	Rh(1′)−S(1′)	2.398(1)
Rh(1)−C(8)	1.869(8)	Rh(1′)−C(8′)	1.886(7)
Rh(1)−C(9)	1.857(5)	Rh(1′)−C(9′)	1.870(5)
Rh(1)−N(2′)	2.083(4)	Rh(1′)−N(2)	2.083(3)
Rh(2)−Cl(1)	2.386(2)	Rh(2′)−Cl(1′)	2.395(1)
Rh(2)−N(1)	2.055(3)	Rh(2′)−N(1′)	2.070(4)
Rh(2)−C(10)	1.834(7)	Rh(2′)−C(10′)	1.814(7)
Rh(2)−C(11)	1.836(8)	Rh(2′)−C(11′)	1.832(7)
Rh(3)−Cl(1)	2.406(1)	Rh(3′)−Cl(1′)	2.427(1)
Rh(3)−S(1)	2.360(1)	Rh(3′)−S(1′)	2.348(1)
Rh(3)−C(12)	2.137(7)	Rh(3′)−C(12′)	2.141(5)
Rh(3)−C(13)	2.168(5)	Rh(3′)−C(13′)	2.177(6)
Rh(3)−C(16)	2.130(4)	Rh(3′)−C(16′)	2.114(6)
Rh(3)−C(17)	2.137(4)	Rh(3′)−C(17′)	2.136(5)
S(1)−C(1)	1.761(4)	S(1′)−C(1′)	1.759(4)
O(1)−C(8)	1.116(10)	O(1′)−C(8′)	1.112(9)
O(2)−C(9)	1.144(6)	O(2′)−C(9′)	1.117(6)
O(3)−C(10)	1.139(10)	O(3′)−C(10′)	1.140(10)
O(4)−C(11)	1.132(12)	O(4′)−C(11′)	1.146(9)
N(1)−C(1)	1.331(5)	N(1′)−C(1′)	1.326(5)
N(1)−C(2)	1.385(5)	N(1′)−C(2′)	1.402(6)
N(2)−C(1)	1.350(5)	N(2′)−C(1′)	1.350(7)
N(2)−C(3)	1.393(5)	N(2′)−C(3′)	1.398(5)
C(2)−C(3)	1.394(6)	C(2′)−C(3′)	1.406(7)
C(12)−C(13)	1.349(11)	C(12′)−C(13′)	1.388(9)
C(16)−C(17)	1.388(9)	C(16′)−C(17′)	1.411(8)
C(8)−Rh(1)−N(2′)	91.2(2)	N(2)−Rh(1′)−C(8′)	90.3(2)
C(8)−Rh(1)−C(9)	90.8(3)	N(2)−Rh(1′)−S(1′)	87.1(1)
S(1)−Rh(1)−N(2′)	86.9(1)	C(8′)−Rh(1′)−C(9′)	90.0(3)
S(1)−Rh(1)−C(9)	91.4(2)	S(1′)−Rh(1′)−C(9′)	92.8(2)
C(10)−Rh(2)−C(11)	88.5(4)	C(10′)−Rh(2′)−C(11′)	88.2(3)
N(1)−Rh(2)−C(10)	92.5(2)	N(1′)−Rh(2′)−C(10′)	94.1(2)
Cl(1)−Rh(2)−C(11)	92.9(3)	Cl(1′)−Rh(2′)−C(11′)	91.3(2)
Cl(1)−Rh(2)−N(1)	86.4(1)	Cl(1′)−Rh(2′)−N(1′)	86.3(1)
C(16)−Rh(3)−C(17)	38.0(2)	C(16′)−Rh(3′)−C(17′)	38.8(2)
C(13)−Rh(3)−C(17)	90.4(2)	C(13′)−Rh(3′)−C(17′)	89.0(2)
C(13)−Rh(3)−C(16)	81.2(2)	C(13′)−Rh(3′)−C(16′)	80.7(2)
C(12)−Rh(3)−C(17)	81.6(2)	C(12′)−Rh(3′)−C(17′)	81.8(2)
C(12)−Rh(3)−C(16)	95.6(2)	C(12′)−Rh(3′)−C(16′)	97.7(2)
C(12)−Rh(3)−C(13)	36.5(2)	C(12′)−Rh(3′)−C(13′)	37.5(2)
S(1)−Rh(3)−C(17)	88.6(1)	S(1′)−Rh(3′)−C(17′)	87.1(1)
S(1)−Rh(3)−C(16)	91.9(1)	S(1′)−Rh(3′)−C(16′)	90.8(2)
Cl(1)−Rh(3)−C(13)	88.5(1)	Cl(1′)−Rh(3′)−C(13′)	89.6(2)
Cl(1)−Rh(3)−C(12)	90.8(2)	Cl(1′)−Rh(3′)−C(12′)	92.5(2)
Cl(1)−Rh(3)−S(1)	94.4(0)	Cl(1′)−Rh(3′)−S(1′)	95.4(1)
Rh(2)−Cl(1)−Rh(3)	83.7(1)	Rh(2′)−Cl(1′)−Rh(3′)	80.3(1)
Rh(1)−S(1)−Rh(3)	95.2(1)	Rh(1′)−S(1′)−Rh(3′)	94.2(0)
Rh(3)−S(1)−C(1)	114.1(1)	Rh(3′)−S(1′)−C(1′)	112.4(2)
Rh(1)−S(1)−C(1)	105.7(2)	Rh(1′)−S(1′)−C(1′)	106.3(1)
Rh(2)−N(1)−C(2)	130.4(3)	Rh(2′)−N(1′)−C(2′)	129.4(3)
Rh(2)−N(1)−C(1)	123.6(3)	Rh(2′)−N(1′)−C(1′)	123.9(3)
C(3)−N(2)−Rh(1′)	128.5(3)	Rh(1)−N(2′)−C(3′)	130.0(3)
C(1)−N(2)−Rh(1′)	126.7(3)	Rh(1)−N(2′)−C(1′)	126.1(3)

arrangements of the bridging ligands and agrees with the frameworks found in the solid state for **2** and for **7**.

NOE experiments to elucidate each particular structure are inoperative because the NOESY spectrum reveals an interconversion between **2a** and **2b**, as detected by negative cross-peaks between the aromatic protons of both isomers (Figure 7). Moreover, this is an equilibrium between tetranuclear species since a 10-fold dilution shows no changes in the relative proportions of **2a**/**2b**, which is in accordance with the molecular weight measurements of **2** in $CHCl_3$ at different concentrations. Therefore, assuming that **2a** possesses the structure found in the solid state, **2b** should be the HT-μ-(1κN,2κS) isomer. The NOESY spectrum also evidences the exchange between all the sites for the olefinic cod protons, as deduced from the negative cross-peaks between them. This involves a process in which a particular Rh(cod) moiety moves between the two coordination

Scheme 2. Proposed Species in Solution for **2**[a]

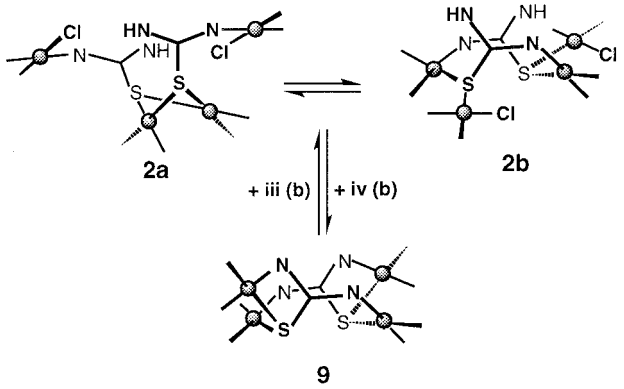

[a] Key: (iii) HCl; (iv) KOH; (b) acetone. Shaded ○< represents the Rh(cod) moiety. Simplified skeletal views of the complexes are shown.

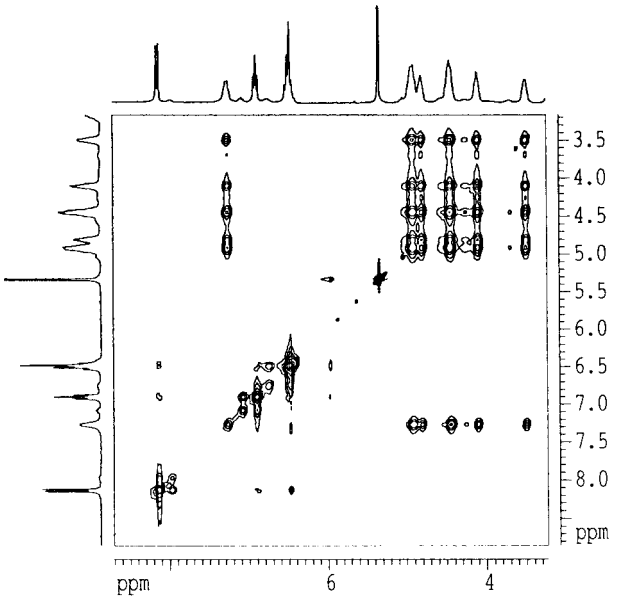

Figure 7. NOESY spectrum at 293 K for the complex [Rh_4(μ-HBzimt)$_2$$Cl_2(cod)_4$] (**2**).

sites in both complexes, which should occur indeed. Thus, an attempt to synthesize the mixed-ligand complex [Rh_4(μ-HBzimt)$_2$-Cl_2(cod)$_2$(tfbb)$_2$] by reaction of [{Rh(μ-HBzimt)(tfbb}$_2$] with [Rh_2(μ-Cl)$_2$(cod)$_2$] in 1:1 molar ratio gives a mixture of complexes showing up to 12 resonances for the NH protons in the ^{1}H NMR spectrum. Up to four symmetrical isomers could be obtained if this synthesis took place in a controlled way, even if an interconversion of the type **2a**/**2b** takes place. However, the above-mentioned 12 signals for the NH protons arise from a mixture of eight isomers having the frameworks of **2a** and **2b**, in which two Rh(tfbb) and two Rh(cod) moieties occupy bridged and terminal cordination positions. The small signals, also observed, should correspond to compounds having three identical Rh(diolefin) fragments. Therefore, a random exchange of Rh(diolefin) fragments occurs, which involves an easy pathway for the migration of the metals in both complexes and their interconversion.

Keys to understanding this behavior are the presence of acidic hydrogens in the tetranuclear complexes, the conformational nonrigidity of the eight-membered ring HT-Rh_2(μ-(1κN,2κS)-HBzimt)$_2$, and the presence of potentially bridging donor atoms such as chlorine and sulfur. The former should give rise to the spontaneous extrusion of hydrogen chloride in **6**, but a simple migration to the close sulfur can easily break the Rh−S bond

and leave an uncoordinated N-donor atom, which can interact easily with the close rhodium centers. It should be noted that the chemical deprotonation of complex **2** is associated with a tremendous change in the bridging framework. Thus, complex **2** gives the neutral complex $[Rh_4(\mu\text{-Bzimt})_2(cod)_4]$ (**9**) by addition of a base (Scheme 2). The connectivity shown by complex **9** is easily achieved from **2b**, since the $Rh_2(\mu_2\text{-}(1\kappa N,2\kappa S)_2)$ dimetallacycle is already preformed, and chelation of two Rh(cod) moieties, already coordinated to sulfur, involves only a change of the conformation of this ring. However, a complicated process is required starting from **2a**. In addition, the opposite reaction of **9** with HCl can easily be understood to give **2a**, assuming that the protonation occurs initially on the sulfur atoms. Therefore, the mobility of the metal fragments occurring in complex **2**, maintaining the two extreme structures in the exchange, can be explained by a mobility of the acidic proton. The conformational nonrigidity is quenched on formation of fused cycles involving the sulfur atoms, as observed for complexes **9** and **10**, which have no acidic protons. Finally, the potentially bridging donor atoms, in particular sulfur, should facilitate the migration of the rhodium centers, and dissociation of a RhCl(diolefin) fragment to give a trinuclear complex cannot be excluded.

On these bases, the surprising preparation of the hexanuclear complex **10** (vide supra) can be now understood and again provides evidence for the mobility of the metal fragments associated to the complexes with an acidic proton. The conformation of the HT-$Rh_2(\mu\text{-}(1\kappa N,2\kappa S)\text{-HBzimt})_2$ ring in **10** does not change in the reaction relative to that of the parent tetranuclear complex **7b**. Therefore, the deprotonation of **7b** by $[\{Rh(\mu\text{-OMe})(cod)\}_2]$ leads to the migration of the $Rh(CO)_2Cl$ fragment bonded to the sulfur to the close nitrogen in a first step, and this sulfur coordinates the Rh(cod)(MeOH) fragment formed in the deprotonation. A further replacement of the cordinated methanol by the chloro ligand renders the final product **10**. This process is consistent with the pathway for the deprotonation of **2b** proposed above.

Complex **5** shows a broad band for the olefinic protons in the ^{1}H NMR spectrum at room temperature but well-defined resonances at low temperature. In this way, the behaviors of complexes **5** and **2** are different. The spectrum in the low-exchange region corresponds to a species having two equivalent $HBzimt^-$ ligands and two types of tfbb ligands, each type giving rise to four inequivalent olefinic protons. Analysis of the H−H COSY spectrum indicates the presence of a C_2 symmetry axis in the molecule, which is confirmed by the four signals for the tertiary protons of the tfbb ligands, since any isomer possessing a plane of symmetry would show six signals for these tertiary protons. Thus, complex **5** could possess a framework of the metals and bridging ligands as found either for **2** or for **7** in the solid state. Comparison of the chemical shifts of the $HBzimt^-$ ligands of **2a**, **2b**, **5**, and **7** shows two distinct patterns, one for **2b**, **5**, and **7** and the other for **2a** and **8**, where the two high-field resonances overlap. This should be due to the distinct disposition of the aromatic ring in complexes of types **2a** and **7**, either close and face to face or further away, respectively. A mutual influence of ring currents between the two aromatic rings should be expected in the first case, producing the distinct patterns observed and thus providing information about the structures of the complexes. Hence, complex **5** should have a framework similar to that of **7**.

Complex **8** decomposes in solution in a few hours. The ^{1}H NMR spectrum shows equivalent bridging ligands and two well-defined signals for the olefinic protons over the range of accessible temperatures. These protons belong to a C═C bond, since the H−H COSY spectrum indicates that they are coupled. Hence, the halves of the cod ligand are equivalent through a plane of symmetry of the molecule. Three ν(CO) bands are observed in the IR spectrum in the solid state and in CH_2Cl_2. These data would be consistent with a structure similar to that found for **2a** but with two eclipsed aromatic rings and the cod ligand attached to one rhodium bridged by the sulfur atoms.

Complex **7** exists as a mixture of two compounds (**7a**, **7b**) whose relative proportion is temperature dependent. Dilution experiments indicate a noticeable variation of the molar ratio between the two species. Thus, a 4-fold dilution of a solution containing 20 mg of **7** in 0.5 mL of $CDCl_3$ produces an increase in **7b** of 270%. This strongly supports a dissociation of **7a** into **7b**, and therefore, the species in solution are in a chemical equilibrium. Variable-temperature ^{1}H NMR studies for a solution of 24 mg of **7** in 0.6 mL of $CDCl_3$ show a **7a**:**7b** ratio of 2.7:1 at 238 K. As the temperature is raised, the relative proportion of **7b** increases rapidly and predominates at 308 K. The equilibrium constant (K_{eq}) over the range 238−308 K fits a linear plot of ln K_{eq} versus $1/T$, which gives $\Delta H = 43.3$ kJ mol^{-1} and $\Delta S = 114.7$ J K^{-1} mol^{-1}. The large positive value observed for ΔS again agrees[4a] with the presence of a dissociative process in solution.

To establish the nuclearity of the species involved in this equilibrium, three independent measurements of the molecular weight for a solution of 20 mg of **7** in 2 mL of $CHCl_3$ give an averaged value of 1215 ± 10. For this concentration, the ^{1}H NMR spectrum in $CDCl_3$ shows 80% of **7b** at room temperature, which gives an averaged molecular weight of 1206, assuming that **7a** and **7b** are octanuclear and tetranuclear complexes, respectively. Therefore, an equilibrium between a possible dinuclear, $[Rh_2(\mu\text{-HBzimt})(\mu\text{-Cl})(CO)_4]$, and tetranuclear species is ruled out. Moreover, comparison of the $^{13}C\{^1H\}$ NMR spectra of the mixture **7a**/**7b** with those of $[Rh_3(\mu\text{-HBzimt})_2(CO)_6]BF_4$ (**11**)[11] and $[Rh_2(\mu\text{-Cl})_2(CO)_4]$ revealed that the latter compounds are not involved in this equilibrium. Furthermore, the IR spectra for very diluted solutions of **7** in hexane, where the low-nuclearity species is dominant, show five ν(CO) absorptions as expected for the tetranuclear complex. Thus, these data support the following equilibrium:

$$\underset{\mathbf{7a}}{[Rh_4(\mu\text{-HBzimt})_2Cl_2(CO)_8]_2} \rightleftharpoons 2\underset{\mathbf{7b}}{[Rh_4(\mu\text{-HBzimt})_2Cl_2(CO)_8]}$$

Complexes **7a** and **7b** show equivalent bridging ligands in the ^{1}H and $^{13}C\{^1H\}$ NMR spectra, the latter displaying two sets of four doublets for the CO groups at low temperature. These spectral data agree with those expected for the equilibrium between the dimer **7a** and the tetranuclear species **7b**. Therefore, the thermodynamic and spectral data support that the tetranuclear complex **7b** associates, even in solution, to give the dimer **7a** and vice versa. The small value found for the dissociation enthalpy ($\Delta H = 43.3$ kJ mol^{-1}) is in agreement with the breaking of four hydrogen bonds.

The lack of an S_n axis for the HT-μ_2-(1kN,2kS) disposition of the $HBzimt^-$ ligands in the tetranuclear species **7b** gives rise to two enantiomers resulting from the eight-membered $Rh_2(N-C-S)_2$ ring (labeled A and B, Chart 2). In addition, each enantiomer could show two different conformations having Λ

(11) $^{13}C\{^1H\}$ NMR ($CDCl_3$, 293 K) for $[Rh_3(\mu\text{-HBzimt})_2(CO)_6]BF_4$, δ: 182.9 (d, $J_{CRh} = 62$ Hz), 180.1 (d, $J_{CRh} = 68$ Hz), 179.7 (d, $J_{CRh} = 75$ Hz) (CO); 146.9 (CS), 140.7 (CN), 133.7 (CN−H), 125.2, 124.6, 115.4, 111.5 (HC) ($HBzimt^-$). $^{13}C\{^1H\}$ NMR ($CDCl_3$, 293 K) for $[Rh_2(\mu\text{-Cl})_2(CO)_4]$, δ: 177.6 (d, $J_{CRh} = 76$ Hz) (CO).

Chart 2. Enantiomers Resulting from the Lack of a Plane of Symmetry in the $Rh_2(N-C-S)_2$ Ring (HT-A, HT-B) and from the Different Helicities (Δ, Λ)

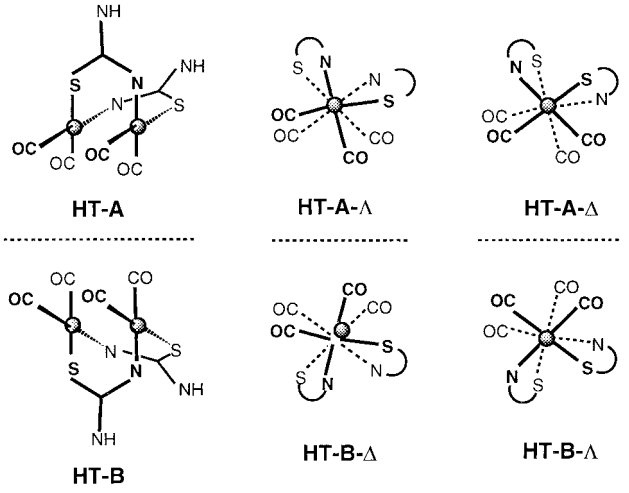

and Δ helicity for a nearly face-to-face disposition of the metal coordination planes in the eight-membered ring. These arise from the twisting of the two planes to avoid an eclipsed conformation of the ligands. Notice that a close disposition of the aromatic rings results for the HT-A-Λ and HT-B-Δ enantiomers, while the distant disposition corresponds to the HT-A-Δ and HT-B-Λ enantiomers. Moreover, the coordination of two $RhCl(CO)_2$ moieties at the sulfur atoms generates two new chiral centers. Thus, six pairs of enantiomers could exist for tetranuclear complex **7b** overall.

The two enantiomers HT-A-Δ and HT-B-Λ found in the solid state, showing *S*,*S* and *R*,*R* configurations at the sulfur atoms, respectively, probably correspond to the more stable for steric reasons, as shown by molecular models. Moreover, a conversion of the conformer HT-A-Δ into HT-A-Λ requires the simultaneous inversion of the configurations at both sulfur atoms to avoid steric crowding. In other words, the twist required for this conversion should be restricted by steric hindrance. Indeed, only two enantiomers are detected by ^1H and $^{13}C\{^1H\}$ NMR spectroscopy. Identical considerations are valid for complex **10**, for which the HT-A-Δ-*S*,*S* and HT-B-Λ-*R*,*R* enantiomers are found in the solid state and only two enantiomers are found in solution.

Conclusions and Remarks

The tetranuclear complex **2** shows tremendous changes in the molecular framework by itself and upon undergoing apparently simple reactions such as the replacement of the ancillary ligands and deprotonation. The equilibrium between complexes **2a** and **2b** could be described as a linkage isomerization, and noticeably, it is observed only for the cod complex. This equilibrium involves a migration of metal fragments. In addition, the structure of complex **2a** has no counterpart, since the related tfbb and carbonyl complexes **5** and **7b** adopt a distinct framework. The structure of **2a** shows two intramolecular hydrogen bonds between a chloro ligand and an acidic proton bonded to nitrogen. This intramolecular hydrogen bonding could assist in the stabilization of the very rare coordination of N−C−S ligands acting as thiolate bridges, but it is not the single cause, because it could also take place in potentially identical structures for **5** and **7b**. On the other hand, the structure found for the carbonyl complex **7** allows for the formation of four intermolecular hydrogen bonds between two tetranuclear complexes, which give rise to a dimer stable even in solution, accounting for the difference with **2a**. However, a dimer like this is not possible for the diolefin complexes because the steric bulk of the olefin ligands prevents the close contacts required to form the intermolecular hydrogen bonding. There is no clear reason for the observed differences between the cod and the tfbb complexes, which should be attributed to the higher π-acidity of the latter ligand.

Experimental Section

Starting Materials and Physical Methods. The benzimidazole-2-thiolate complexes were prepared as previously described.[2] Standard literature procedures were used to prepare $[M_2(\mu\text{-Cl})_2(\text{diolefin})_2]$,[12] [M(acac)(diolefin)],[13] and $[Rh_2(\mu\text{-OMe})_2(\text{cod})_2]$.[14] All solvents were dried and distilled before use by standard methods, and the new complexes were prepared under an argon atmosphere using Schlenk techniques. Molecular weights were determined with a Knauer osmometer using chloroform solutions. Carbon, hydrogen, nitrogen, and sulfur analyses were performed in a Perkin-Elmer 2400 microanalyzer. IR spectra were recorded with a Nicolet-IR 550 (4000−400 cm^{-1}) spectrophotometer with the bands calibrated against the sharp peak (1601.4 cm^{-1}) of a polystyrene film. Mass spectra were recorded in a VG Autospec double-focusing mass spectrometer operating in the FAB^+ mode. ^1H and $^{13}C\{^1H\}$ spectra were recorded on Varian UNITY 300 and Bruker ARX 300 spectrometers operating at 299.95 and 300.13 MHz, respectively, for ^1H. Chemical shifts are referenced to $SiMe_4$. H−H COSY spectra were registered with the COSYGR pulse program on the Bruker spectrometer using 256 individual FID's with four acquisitions per FID. NOESY spectra were recorded with the NOESYTP pulse program (phase sensitive, to differentiate the positive from the negative cross-peaks) on the Bruker spectrometer using 256 individual FID's with 32 acquisitions per FID.

Preparations of the Complexes. $[Rh_4(\mu\text{-HBzimt})_2Cl_2(cod)_4]$ (2). Method A. Solid $[Rh_2(\mu\text{-Cl})_2(cod)_2]$ (48 mg, 0.1 mmol) was added to a yellow solution of $[Rh_2(\mu\text{-HBzimt})_2(cod)_2]$ (70 mg, 0.1 mmol) in acetone (15 mL) to give immediately a red solution, which was allowed to stand overnight at −40 °C. The deposited red microcrystals were collected by filtration, washed with cold diethyl ether (5 mL), and vacuum-dried. Yield: 96 mg (82%).

Method B. An acetone solution (25 mL) of [Rh(acac)(cod)] (93 mg, 0.3 mmol) was allowed to diffuse through a porous frit into a solution, in the same solvent (25 mL), of $[RhCl(H_2Bzimt)(cod)]$ (120 mg, 0.3 mmol). Red crystals, suitable for diffraction studies, were formed at the porous frit in 2 days which were separated by decantation, washed with cold diethyl ether, and vacuum-dried. A second crop of crystals were obtained by evaporation of the solution and addition of diethyl ether. Overall yield: 144 mg (82%).

IR (Nujol): $\nu(N-H) = 3120\ cm^{-1}$. ^1H NMR data ($CDCl_3$, 218 K) (obtained from H−H COSY analysis) are as follows. For **2a**, δ: 11.25 (m, 2H, NH), 8.10 (d, 6 Hz, 2H), 6.85 (m, 2H), 6.46 (m, 4H) ($HBzimt^-$); 7.20 (m, 2H), 4.84 (m, 4H), 4.78 (m, 2H), 4.38 (m, 4H), 3.96 (m, 2H), 3.42 (m, 2H) (=CH, cod); 3.13 (m, 2H), 2.75 (m, 6H), 2.52 (m, 2H), 2.34 (m, 6H), 2.26 (m, 2H), 2.05 (m, 6H), 1.93 (m, 2H), 1.81 (m, 2H), 1.61 (m, 2H), 1.47 (m, 2H) ($>CH_2$, cod). For **2b**, δ: 11.41 (m, 2H, NH), 7.86 (d, 8.2 Hz, 2H), 7.04 (t, 8.2 Hz, 2H), 6.67 (t, 8.5 Hz, 2H), 6.35 (d, 8.5 Hz, 2H) ($HBzimt^-$); 6.85 (m, 2H), 5.00 (m, 2H), 4.48 (m, 4H), 4.07 (m, 2H), 3.88 (m, 2H), 3.64 (m, 4H) (=CH, cod); the remaining methylenic cod protons are overlapped with those of the isomer **2a** except the exo proton coupled with the olefinic proton at $\delta = 6.85$ which appears at $\delta = 2.95$.$^{13}C\{^1H\}$ NMR ($CDCl_3$, 293 K) for **2a**, δ: 150.7 (CS), 141.4 (CN), 133.9 (CN−H), 122.8, 121.6, 116.1, 111.5 (HC) ($HBzimt^-$); 88.1 (d, $^1J_{CRh} = 12$ Hz), 87.5 (d, $^1J_{CRh} = 14$ Hz), 85.9 (d, $^1J_{CRh} = 12$ Hz), 83.8 (d, $^1J_{CRh} = 12$ Hz), 82.3 (d, $^1J_{CRh} = 13$ Hz), 81.3 (d, $^1J_{CRh} = 12$ Hz), 76.8 (d, $^1J_{CRh} = 13$ Hz), 75.2 (d, $^1J_{CRh}$

(12) (a) Giordano, G.; Crabtree, R. H. *Inorg. Synth.* **1979**, *19*, 218. (b) Herde, J. L.; Lambert, J. C.; Senoff, C. V. *Inorg. Synth.* **1974**, *15*, 18.
(13) (a) Bonati, F.; Wilkinson, G. *J. Chem. Soc.* **1964**, 3156. (b) Robinson, S. R.; Shaw, B. L. *J. Chem. Soc.* **1965**, 4997.
(14) Chatt, J.; Venanzi, L. M. *J. Chem. Soc.* **1957**, 4735.

Table 4. Crystallographic Data for Complexes **2**, **7**, and **10**

	2	**7**	**10**
formula	$C_{46}H_{58}Cl_2N_4Rh_4S_2$	$C_{22}H_{10}Cl_2N_4O_8Rh_4S_2 \cdot CH_2Cl_2$	$C_{38}H_{32}Cl_2N_4O_8Rh_6S_2 \cdot 1.5CH_2Cl_2$
mol wt	1213.64	1089.92	1552.55
cryst syst	monoclinic	tetragonal	triclinic
space group	*C*2/*c*	$I4_1/a$	$P\bar{1}$
radiation (λ, Å)	graphite-monochromated Mo Kα (0.710 73)		
a, Å	26.021(7)	21.389(3)	16.967(4)
b, Å	13.741(4)	21.389(3)	14.289(3)
c, Å	13.123(4)	29.359(6)	11.872(2)
α, β, γ, deg	105.31(2)		71.90(2), 68.24(2), 77.60(2)
V, Å^3	4526(2)	13431(4)	2525(1)
Z	4	16	2
D_{calcd}, g cm^{-3}	1.781	2.156	2.042
μ, cm^{-1}	16.81	24.24	23.14
R^a	0.0264	0.0463	0.0359
$R_w{}^b$	0.0321	0.1253	0.0474

^{a} $R = \sum||F_o| - |F_c||/\sum|F_o|$. ^{b} $R_w = [\sum w(|F_o| - |F_c|)^2/\sum w(F_o)^2]^{1/2}$.

= 14 Hz) (=CH, cod); 33.5, 33.0, 32.5, 31.8, 30.5, 30.2, 30.0, 29.3 (>CH_2, cod). Anal. Calcd for $C_{46}H_{58}Cl_2N_4S_2Rh_4$: C, 45.52; H, 4.82; N, 4.62; S, 5.28. Found: C, 45.86; H, 4.63; N, 4.65; S, 5.22. MS (FAB$^+$), *m*/*z*: 931 ([Rh_3(μ-HBzimt)$_2$(cod)$_3$]$^+$, 28%), 571 ([Rh_2(μ-HBzimt)$_2$(cod)$_2$]$^+$, 100%). Molecular weight: calcd for [Rh_4(μ-HBzimt)$_2$$Cl_2(cod)_4$], 1214; found, 1207.

[Rh_3(μ-HBzimt)$_2$(cod)$_3$]Cl (3). A methanolic suspension (5 mL) of [Rh_2(μ-Cl)$_2$(cod)$_2$] (24 mg, 0.05 mmol) was added dropwise to a suspension of [Rh_2(μ-HBzimt)$_2$(cod)$_2$] (70 mg, 0.1 mmol) in methanol (5 mL). Purple microcrystals deposited after 10 min of stirring, which were filtered off, washed with diethyl ether, and vacuum-dried. Yield: 82 mg (85%). ^{1}H NMR (CD_3OD, 293 K), δ: 7.70 (d, 8.2 Hz, 2H), 6.85 (t, 2H, 8.2 Hz), 6.60 (t, 2H, 8.1 Hz), 6.50 (d, 2H, 7.9 Hz) (HBzimt$^-$); 5.60 (m, 2H), 5.33 (m, 2H), 4.44 (m, 2H), 4.25 (m, 2H), 3.90 (m, 2H), 3.63 (m, 2H) (=CH, cod); 3.18 (m, 2H), 2.98 (m, 1H), 2.42 (m, 2H), 2.32 (m, 2H), 2.22 (m, 2H), 2.10 (m, 1H), 1.78 (m, 1H), 1.65 (m, 1H) (>CH_2, cod). Anal. Calcd for $C_{38}H_{46}ClN_4S_2Rh_3$: C, 47.22; H, 4.80; N, 5.80; S, 6.62. Found: C, 47.13; H, 4.51; N, 5.66; S, 6.55. MS (FAB$^+$), *m*/*z*: 931 ([Rh_3(μ-HBzimt)$_2$(cod)$_3$]$^+$, 100%).

[Rh_4(μ-HBzimt)$_2$$Cl_2$(tfbb)$_4$] (5) was prepared as a green microcrystalline solid from [RhCl(H_2Bzimt)(tfbb)] (prepared in situ by addition of H_2Bzimt (30 mg, 0.2 mmol) to a suspension of [Rh_2(μ-Cl)$_2$(tfbb)$_2$] (73 mg, 0.1 mmol) in acetone) and [Rh(acac)(tfbb)] (43 mg, 0.1 mmol) by the method B described above for **3**. Yield: 140 mg (83%). IR (Nujol): ν(N−H) = 3160 cm^{-1}. ^{1}H NMR ($CDCl_3$, 218 K), δ: 11.73 (s, 2H, NH), 8.02 (d, 8.5 Hz, 2H), 7.14 (t, 2H, 8.0 Hz), 6.77 (t, 2H, 7.5 Hz), 6.46 (d, 2H, 7.7.5 Hz) (HBzimt$^-$); 6.48 (br s, 2H), 5.54 (m, 2H), 5.40 (m, 2H), 3.78 (br s, 2H) (>CH, tfbb); 6.05 (m, 2H), 5.71 (m, 2H), 4.38 (m, 2H), 4.33 (m, 2H), 4.27 (m, 2H), 3.78 (m, 4H), 2.89 (m, 2H) (=CH, tfbb). Anal. Calcd for $C_{62}H_{34}Cl_2F_{16}N_4S_2Rh_4$: C, 44.19; H, 2.03; N, 3.32; S, 3.80. Found: C, 43.86; H, 2.20; N, 3.39; S, 3.66. MS (FAB$^+$), *m*/*z*: 1285 ([Rh_3(μ-HBzimt)$_2$(tfbb)$_3$]$^+$, 100%).

[Ir_4(μ-HBzimt)$_2$$Cl_2(cod)_4$] (6) was prepared, as a dark green microcrystalline solid, from [IrCl(H_2Bzimt)(cod)] (70 mg, 0.14 mmol) and [Ir(acac)(cod)] (57 mg, 0.14 mmol) by the method B described above for **3**. Yield: 77 mg (68%). IR (Nujol): ν(N−H) = 3100 cm^{-1}. Anal. Calcd for $C_{46}H_{58}Cl_2N_4S_2Ir_4$: C, 35.17; H, 3.72; N, 3.57; S, 4.08. Found: C, 35.64; H, 3.40; N, 3.53; S, 4.10. MS (FAB$^+$), *m*/*z*: 1199 ([Ir_3(μ-HBzimt)$_2$(cod)$_3$]$^+$, 100%). Complex **6** gives orange solutions in $CDCl_3$ whose ^{1}H NMR and ^{13}C{^{1}H} NMR spectra correspond to [Ir_4(μ-Bzimt)$_2$(cod)$_4$].

[Rh_4(μ-HBzimt)$_2$$Cl_2(CO)_8$] (7). Dry carbon monoxide was bubbled through a concentrated solution of **3** (121 mg, 0.1 mmol) in deoxygenated dichloromethane (5 mL). After 15 min, the initially red solution became wine-red, and hexane (5 mL) was added. Bubbling was continued for 2 h, and small amounts of hexane were added to complete the crystallization of **7**, which was filtered off, washed with cold hexane (3 mL), and vacuum-dried. Yield: 85 mg (80%). IR (Nujol): ν(N−H) = 3140 cm^{-1}. IR (hexane): ν(CO) = 2102 (m), 2089 (vs), 2078 (w), 2036 (s), 2023 (m), 2006 (w) cm^{-1}. ^{1}H NMR data ($CDCl_3$, 218 K) are as follows. For **7a**, δ: 11.62 (s, 2H, NH), 7.67 (d, 7.9 Hz, 2H), 7.35 (t, 2H, 7.8 Hz), 7.12 (t, 2H, 8.1 Hz), 6.37 (d, 2H, 7.9 Hz) (HBzimt$^-$). For **7b**, δ: 11.75 (s, 2H, NH), 7.64 (d, 6.8 Hz, 2H), 7.07 (t, 2H, 7.3 Hz), 6.74 (t, 2H, 7.6 Hz), 6.16 (d, 2H, 8.1 Hz) (HBzimt$^-$). ^{13}C{^{1}H} NMR data ($CDCl_3$, 218 K) are as follows. For **7a**, δ: 184.2 (d, J_{CRh} = 63 Hz), 180.0 (d, J_{CRh} = 73 Hz), 180.5 (d, J_{CRh} = 64 Hz), 179.5 (d, J_{CRh} = 61 Hz) (CO); 153.4 (CS), 139.8 (CN), 132.0 (CN−H), 125.2, 123.3, 115.9, 111.3 (HC) (HBzimt$^-$). For **7b**, δ: 183.1 (d, J_{CRh} = 65 Hz), 180.3 (d, J_{CRh} = 58 Hz), 180.0 (d, J_{CRh} = 70 Hz), 179.4 (d, J_{CRh} = 74 Hz) (CO); 147.6 (CS), 139.7 (CN), 133.0 (CN−H), 125.2, 122.8, 115.9, 110.0 (HC) (HBzimt$^-$). Anal. Calcd for $C_{22}H_{10}Cl_2N_4O_8S_2Rh_4$: C, 26.29; H, 1.00; N, 5.57; S, 6.38. Found: C, 26.53; H, 1.23; N, 5.39; S, 6.21. MS (FAB$^+$), *m*/*z*: 775 ([Rh_3(μ-HBzimt)$_2$(CO)$_6$]$^+$, 100%). Molecular weight: calcd for [Rh_4(μ-HBzimt)$_2$$Cl_2(CO)_4$], 1005; found, 1215.

[Rh_4(μ-HBzimt)$_2$$Cl_2$(cod)(CO)$_6$] (8). Dry carbon monoxide was bubbled through a suspension of **3** (121 mg, 0.1 mmol) in deoxygenated diethyl ether (15 mL). The starting material dissolved in 10 min, and CO bubbling was continued for a further 20 min. Slow evaporation of the solvent, under an Ar atmosphere, led to the formation of pink needles corresponding to **8**, which were filtered off, washed with cold hexane (3 mL), and vacuum-dried. Yield: 80 mg (75%). IR (Nujol): ν(N−H) = 3132 cm^{-1}. IR (CH_2Cl_2): ν(CO) = 2079 (vs), 2025 (s), 1996 (m) cm^{-1}. ^{1}H NMR ($CDCl_3$, 293 K), δ: 11.43 (s, 2H, NH), 7.79 (d, 8.2 Hz, 2H), 6.99 (m, 2H), 6.71 (m, 4H) (HBzimt$^-$); 5.07 (m, 2H), 3.71 (m, 2H) (=CH, cod); 2.87 (m, 2H), 2.50 (m, 2H), 2.23 (m, 2H), 1.83 (m, 2H) >CH_2, cod). Anal. Calcd for $C_{28}H_{22}Cl_2N_4O_6S_2Rh_4$: C, 31.81; H, 2.10; N, 5.30; S, 6.06. Found: C, 31.60; H, 1.95; N, 5.33; S, 5.91.

[Rh_6(μ-Bzimt)$_2$(μ-Cl)$_2$(cod)$_2$(CO)$_8$] (10). Solid [Rh_2(μ-OMe)$_2$(cod)$_2$] (48.4 mg, 0.1 mmol) was added to a solution of [Rh_4(μ-HBzimt)$_2$$Cl_2(CO)_8$] (**7**) (100.5 mg, 0.1 mmol) in 15 mL of dichloromethane. The resulting red solution was stirred for 30 min and then was concentrated to ca. 2 mL. Slow addition of heptane gave **10** as dark red needles, which were filtered off, washed with heptane, and vacuum-dried. Yield: 114 mg (80%). IR (CH_2Cl_2): ν(CO) = 2087 (m), 2078 (vs), 2065 (w), 2027 (s), 2013 (s) cm^{-1}. ^{1}H NMR ($CDCl_3$, 293 K), δ: 7.63 (m, 4H), 7.20 (m, 4H) (HBzimt$^-$); 5.08 (m, 2H), 4.42 (m, 4H), 3.73 (m, 2H) (=CH, cod); 3.01 (m, 2H), 2.72 (m, 2H), 2.36 (m, 6H), 2.09 (m, 2H), 1.74 (m, 4H) (>CH_2, cod).^{13}C{^{1}H} NMR ($CDCl_3$, 218 K), δ: 185.0 (d, J_{CRh} = 62 Hz), 184.7 (d, J_{CRh} = 62 Hz), 182.1 (d, J_{CRh} = 72 Hz), 180.8 (d, J_{CRh} = 80 Hz) (CO); 158.7 (CS), 144.7, 143.7 (CN); 121.8, 121.6, 114.6, 113.3 (HC) (Bzimt^{2-}); 89.6 (d, J_{CRh} = 11 Hz), 87.3 (d, J_{CRh} = 11 Hz), 81.8 (d, J_{CRh} = 14 Hz), 75.1 (d, J_{CRh} = 16 Hz) (=CH, cod); 34.5, 33.4, 29.4, 28.0 (>CH_2, cod). Anal. Calcd for $C_{38}H_{32}Cl_2N_4O_8S_2Rh_6$: C, 32.03; H, 2.26; N, 3.93; S, 4.50. Found: C, 32.46; H, 2.16; N, 3.94; S, 4.23. MS (FAB$^+$), *m*/*z*: 1423 (for ^{35}Cl) (M$^+$, 55%).

Crystal Structure Determination of Complexes 2, 7·CH_2Cl_2, and 10·1.5CH_2Cl_2. Selected crystallographic data for complexes **2**, **7**, and **10** are listed in Table 4. Data were collected at room temperature (22

°C, **2** and **10**) and at 173K (**7**) on Siemens AED (**2**), Siemens-Stoe (**7**), and Philips PW 1100 (**10**) four-circle diffractometers using graphite-monochromated Mo Kα radiation. Crystal dimensions were 0.15 × 0.17 × 0.26 (**2**), 0.20 × 0.25 × 0.38 (**7**), and 0.25 × 0.31 × 0.40 (**10**) mm. All reflections with θ in the ranges 3−27 (**2**), 3−25 (**7**), and 3−30° (**10**) were measured using $\theta/2\theta$ (**2**, **10**) and $\omega/2\theta$ (**7**) scans; of 4951 (**2**), 5901 (**7**), and 14 621 (**10**) independent reflections, 2764 (**2**) and 9258 (**10**), having $I > 2\sigma(I)$, were considered observed and used in the analysis. In the case of **7**, 5897 reflections were included in the refinement. One (**2** and **10**) or three (**7**) standard reflections were monitored every 100 measurements; no significant decay was noticed over the time of data collection. Intensities were corrected for Lorentz and polarization effects. As all three single-crystal samples exhibited small and homogeneous crystal dimensions, with μr factors under 0.37, no absorption correction was carried out.

The structures were solved by direct and Fourier methods and refined by full-matrix (**2**) or blocked full-matrix (**10**) least-squares calculations based on F and full-matrix least-squares calculations based on F^2 (**7**), first with isotropic displacement parameters and then with anisotropic thermal parameters for the non-hydrogen atoms. In **7** and in **10**, a CH_2Cl_2 molecule of solvation was found disordered and distributed in two positions of equal occupancy. In **2**, all hydrogen atoms except four (of the $-CH_2$ groups) were found in the ΔF final map and refined isotropically; these four were placed at their geometrically calculated positions (C−H = 0.96 Å) and refined riding on the corresponding carbon atoms (with isotropic thermal parameters); in **7** and **10**, all hydrogen atoms were placed at their geometrically calculated positions (C−H = 0.96 Å) and refined riding on the corresponding carbon atoms (with isotropic thermal parameters), except the eight olefinic hydrogens in **10**, which were found and refined isotropically. The final cycles of refinement were carried out on the bases of 366 (**2**), 432 (**7**), and 652 (**10**) variables. The highest remaining peaks in the final difference maps were equivalent to about 0.53 (**2**), 1.43 (**7**), and 1.06 (**10**) e/Å^3. In the final cycles of refinement, a weighting scheme $w = [\sigma^2(F_o) + gF_o^2]^{-1}$ was used for **2** and **10**; at convergence, the g values were 0.0003 (**2**) and 0.0029 (**10**). Final R and R_w values were 0.0264 and 0.0321 (**2**) and 0.0359 and 0.0474 (**10**). In the case of **7**, the calculated weighting scheme was $1/[\sigma^2(F_o^2) + (0.0843P)^2 + 52.11P]$, where $P = (F_o^2 + 2F_c^2)/3$. Final agreement factors for **7** were $R(F) = 0.046$ ($F^2 \geq 2\sigma(F^2)$, 5197 reflections) and $R_w(F^2) = 0.125$ for all data. The analytical scattering factors, corrected for the real and imaginary parts of anomalous dispersion, were taken from ref 15. All calculations were carried out on the GOULD POWERNODE 6040 and ENCORE 91 computers of the Centro di Studio per la Strutturistica Diffrattometrica del CNR, Parma, Italy, using the SHELX-76 and SHELXS-86 systems of crystallographic computer programs[16] (**2** and **10**) or the SHELXL93[17] package (**7**).

Acknowledgment. We wish to thank the Dirección General de Investigación Científica y Técnica (DGICYT) for financial support (Projects PB95-221-C1 and PB94-1186), Consiglio Nazionale delle Ricerche (CNR), and Consejo Superior de Investigaciones Cientificas (CSIC) for a collaboration project and the EU Human Capital and Mobility Program (CT93-0347) for a fellowship to A.J.E.

Supporting Information Available: X-ray crystallographic files, in CIF format, for complexes **2**, **7**, and **10** are available on the Internet only. Access information is given on any current masthead page.

IC971376P

(15) *International Tables for X-ray Crystallography*; Kynoch Press: Birmingham, England, 1974; Vol. IV.
(16) Sheldrick, G. M. *SHELX-76: Program for crystal structure determination*; University of Cambridge: England, 1976. Sheldrick, G. M. *SHELXS-86: Program for the solution of crystal structures*; University of Göttingen: Germany, 1986.
(17) Sheldrick, G. M. *SHELXL-93*; University of Göttingen: Germany, 1993.